JOURNAL OF MATERIALS SCIENCE 22 (1987) 3851–3863

Ageing characteristics of Al–2.5% Li rapidly solidified alloy

F. H. SAMUEL
Central Metallurgical Research and Development Institute, El-Tabbin, Helwan, PO Box Iron and Steel, Cairo, Egypt

G. CHAMPIER
Laboratoire de Physique du Solide, Ecole des Mines, Parc de Saurupt, 54042 Nancy Cedex, France

The present work was performed on an Al–2.5 wt% Li alloy produced by melt spinning. The ribbons were aged in the temperature range 160 to 310° C for times between 1 min and 120 h. The kinetics of coarsening of $\delta'(Al_3Li)$ and $\delta(AlLi)$ phase particles were investigated using transmission electron microscopy and hardness measurements. The results show that coarsening of $\delta'(Al_3Li)$ follows a simple linear relation with the cube root of time, whereas coarsening of $\delta(AlLi)$ does not follow the same trend. We believe that the $\delta(AlLi)$ phase nucleates at the $\delta'(Al_3Li)$/matrix interface and grows by the dissolution of the nearby $\delta'(Al_3Li)$ particles. The mechanical properties of the powder metallurgy alloy show that a large volume fraction of PFZ contributes to the alloy ductility, ~11%, in the aged condition. Also, the yield strength is greatly improved due to refinement effects enhanced by rapid solidification.

1. Introduction

In the past few years, the importance of adding lithium (up to 3 wt %) to high-strength aluminium for aeronautical purposes has received a great deal of attention. Each weight per cent of lithium added to pure aluminium reduces its density by about 3% and increases the elastic modulus by about 6% [1]. In the region of interest of the phase diagram [2] the principal phases are α(Al–Li solid solution), δ(AlLi equilibrium intermetallic) and $\delta'(Al_3Li$ metastable ordered phase). According to the theory of Lifshitz, Slyozov and Wagner (discussed in [2]), the coarsening of δ'-phase particles on ageing follows a linear relationship with the cube root of ageing time [3]. The equilibrium δ-phase has been reported [4] to nucleate heterogeneously after a relatively long ageing time (at temperatures below the δ' solvus line) and invariably results in the dissolution of the surrounding δ' matrix. From the mechanical properties point of view, addition of lithium increases both the strength and stiffness of the aluminium alloys due to precipitation of a high volume fraction of δ'-phase particles (homogeneous precipitation). Unfortunately, the fracture toughness of Al–Li alloys is unacceptably low for many industrial applications. This is coupled with a marked loss of ductility during ageing [5].

The work reported here was directed at determining the influence of rapid solidification on the coarsening of the δ' particles, the growth of the precipitate free zone (PFZ) and the formation of δ-phase particles in an Al–2.5 wt % Li alloy by means of transmission electron microscopy. For the purpose of studying their effect on the mechanical properties, another alloy was prepared by powder metallurgy technique using centrifugal atomization followed by degassing and hot extrusion.

2. Experimental procedure

The experiments were performed on an Al–Li alloy (containing 2.56% Li) produced by melt spinning (MS). The alloy was prepared from high-purity aluminium and lithium metals under an inert atmosphere of helium. The alloy was spun into ribbons by conventional melt spinning using a copper disc as the rotating chill substrate. The melt spinning was done in a chamber under a helium atmosphere. The ribbon width was typically 1500 μm with a thickness lying in the range 30 to 40 μm. All the ribbons were aged without prior solution heat treatment. The heat-treatment regime is shown in Table I.

Detailed metallographic examinations were made on the ribbons at different conditions, employing standard transmission electron microscopy (TEM). The foils were investigated in an electron microscope operating at 200 kV and various specimen inclinations were adopted. Microhardness measurements were done on the long edges of the ribbons using loads varying between 5 and 15 g depending on the ribbon hardness.

Another set of experiments were carried out on the same alloy in the form of consolidated powders (lithium content was found to be 2.46%). The powder was prepared by conventional centrifugal atomizing process to obtain high-speed convective cooling. These powders were degassed under vacuum (10^{-4} torr) for 24 h at 200° C, then extruded at 420° C after annealing at this temperature for 1 h. The as-extruded rods were solution heat-treated at 540° C for 0.5 h

0022–2461/87 $03.00 + .12

TABLE I TEM and hardness data

(a) Ageing temperature 25° C

	Ageing time		
	0 h	1 week	3 months
δ' diameter (nm)	5	5–7	10
δ' (vol %)	22	16–18	19–21
HV	45	45	50

(b) Ageing temperature 160° C

	Ageing time (h)					
	1	8	16	36	100	120
$\omega/2$ (μm)	0.02	–	0.035	0.052	0.07	0.076
PFZ (vol %)	3	–	6–7	10	13	14
δ' diameter (nm)	8	–	20	26	35	40
δ' (vol %)	26	–	27	29	31	33
HV	60	–	80	85	85	85

(c) Ageing temperature 200° C

	Ageing time (h)				
	1	16	36	100	120
$\omega/2$ (μm)	0.125	0.300	0.42	0.55	0.65
PFZ (vol %)	12	24	35	45	50
δ' diameter (nm)	10–12	40	52	60	76
δ' (vol %)	24	32	37	42	47
HV	80	120	100	90	80

(d) Ageing temperature 240° C

	Ageing time (h)					
	1	8	16	36	100	120
$\omega/2$ (μm)	0.155	–	0.46	0.55	0.78	–
PFZ (vol %)	14	–	33	43	57	62
δ' diameter (nm)	22	–	60	75	95	108
δ' (vol %)	25	–	36	40	49	50

(e) Ageing temperature 280° C

	Ageing time (h)							
	0.25	0.5	1	2	8	16	36	100
$\omega/2$ (μm)	0.07	0.08	0.105	0.12	0.14	0.17	–	–
PFZ (vol %)	?	?	?	?	?	?	–	–
δ' diameter (nm)	25	31	35	43	21	14	5	not visible
δ diameter (nm)	87	140	160	210	187–220	150–250	150–300	270–400
No. grain	241	458	1110	995	1853	2170	2327	
Form	spherical	spherical	spherical	spherical	spherical	spherical		spherical + rod
HV	55	70	80	70	65	60	–	–

(f) Ageing temperature 300° C

	Ageing time (min)				
	1	5	15	30	60
$\omega/2$ (μm)	0.07	0.08	0.10	NO PFZ or δ'	
δ' diameter (nm)	12	14	17		
δ diameter (nm)	150	240	350	480	1200
No. grain	3210	3260	3220	–	–
Form	spherical			spherical, plates, rods	mostly plates

prior ageing at 200 and 220° C (for practical applications). Round tensile specimens (4 mm diameter and 18 mm gauge length) were machined from the heat-treated rods and tested in a Universal Tensile Testing Machine at room temperature, at a constant strain rate of $6 \times 10^{-4}\,\text{sec}^{-1}$. The strain was measured by means of an extensometer of 10 mm gauge length.

3. Results and discussion

3.1. Metallography

3.1.1. Grain-boundary condition

Figs 1a to e represent the condition of the grain boundary as a function of the ageing temperature. In Fig. 1a, the microstructure reveals the refinement effect of the high freezing rate used to produce the present ribbons. The grains are of high-angle misorientation with no visible coarse precipitation on the grain boundary. The average grain size in this case is almost 2 to 3 μm (about 150 μm in the case of classical casting). Jensrud and Ryum [6] have studied the effect of the temperature of the quenching bath on the density of δ(AlLi) particles in an Al–3 wt % solid state alloy. Their study shows that even quenching into liquid nitrogen at -196° C does not prevent the appearance of δ-phase particles on the high-angle grain boundaries. Thus the absence of such an observation in the present work may be attributed to (a) the large surface of grain boundaries that results in decreasing the concentration of lithium atoms at the grain boundaries and, thus, does not favour formation of the said phase, (b) the fact that the lithium concentration is even in the melt-spun alloy, (c) the speed of the quench at critical stages in the cooling, and (d) the use of lower lithium concentration (2.56%) compared with that of 3% used by Jensrud and Ryum [6].

Ageing of Al–Li alloys at or above a critical temperature results in preferential precipitation and coarsening of the equilibrium AlLi(δ)-phase at the grain boundaries, leading to the development and growth of precipitate free zones (PFZs) [4]. Although a theoretical basis has not yet been found, it is known that the reason for PFZ formation differs for different alloy systems. Fig. 1b exhibits the grain boundaries after ageing the present ribbons at 200° C (the temperature at which most of the earlier studies have been carried out) for 36 h. As can be seen, though a wide PFZ area is decorating the grain boundaries, no signs of δ(AlLi) or $\delta'(Al_3Li)$ particles are visible (for

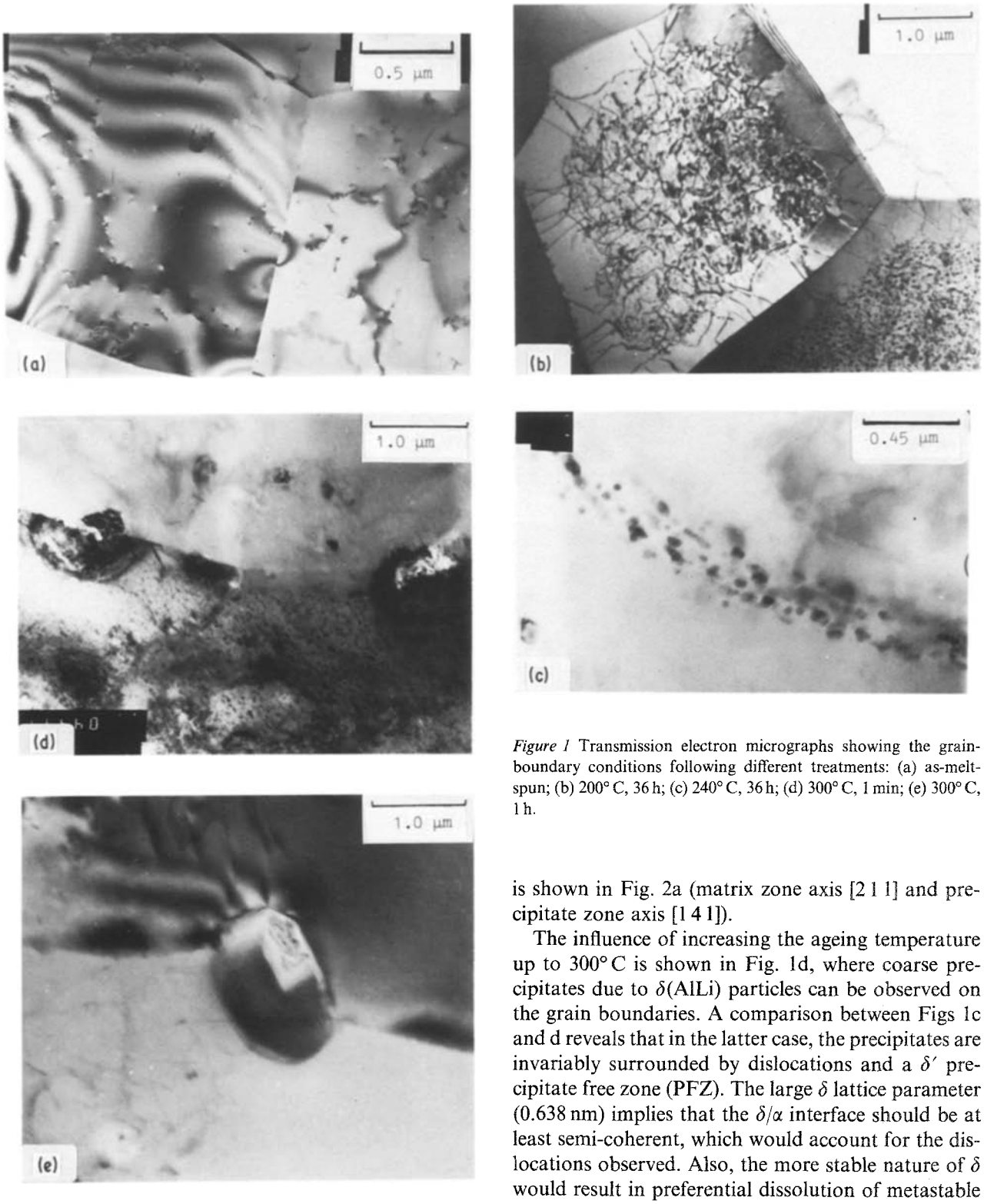

Figure 1 Transmission electron micrographs showing the grain-boundary conditions following different treatments: (a) as-melt-spun; (b) 200° C, 36 h; (c) 240° C, 36 h; (d) 300° C, 1 min; (e) 300° C, 1 h.

comparison see [3]). We believe that the present observation of the PFZ at 200° C can be discussed on the basis of the vacancy concentration model [7]. According to this model, for the present MS alloy, a PFZ will chiefly occur because of loss of vacancies at grain boundaries and homogeneous nucleation is likely to take place with excess vacancies. As a consequence of this process, the PFZ may have widths up to 1 μm, independent of the initial grain size.

Coarse precipitates due to δ(AlLi) phase at the grain boundaries was first observed at 240° C after annealing for times as long as 36 h, Fig. 1c. A typical selected-area diffraction pattern from the δ precipitate is shown in Fig. 2a (matrix zone axis [2 1 1] and precipitate zone axis [1 4 1]).

The influence of increasing the ageing temperature up to 300° C is shown in Fig. 1d, where coarse precipitates due to δ(AlLi) particles can be observed on the grain boundaries. A comparison between Figs 1c and d reveals that in the latter case, the precipitates are invariably surrounded by dislocations and a δ' precipitate free zone (PFZ). The large δ lattice parameter (0.638 nm) implies that the δ/α interface should be at least semi-coherent, which would account for the dislocations observed. Also, the more stable nature of δ would result in preferential dissolution of metastable δ' [8]. The effect of increasing the annealing time from 1 min (Fig. 1d) to 1 h is seen in Fig. 1e. It is evident from this micrograph that the δ-precipitate particle is rod-shaped and $\sim 0.5\,\mu$m in diameter and $\sim 1\,\mu$m in length. The δ/α interface is incoherent with a sharp boundary. The occurrence of δ causes a change in the grain boundary with a zone of plastic deformation as inferred from the presence of dislocations at the δ/α interface. The corresponding electron diffraction pattern Fig. 2b indicates the following relations:

$$(2\,\bar{1}\,1)_{\delta} \parallel (2\,1\,1)_{\alpha\text{-Al}}$$

$$[\bar{1}\,\bar{1}\,1]_{\delta} \parallel [0\,\bar{1}\,1]_{\text{Al}}$$

$$[0\,1\,1]_{\delta} \parallel [\bar{1}\,1\,1]_{\text{Al}}$$

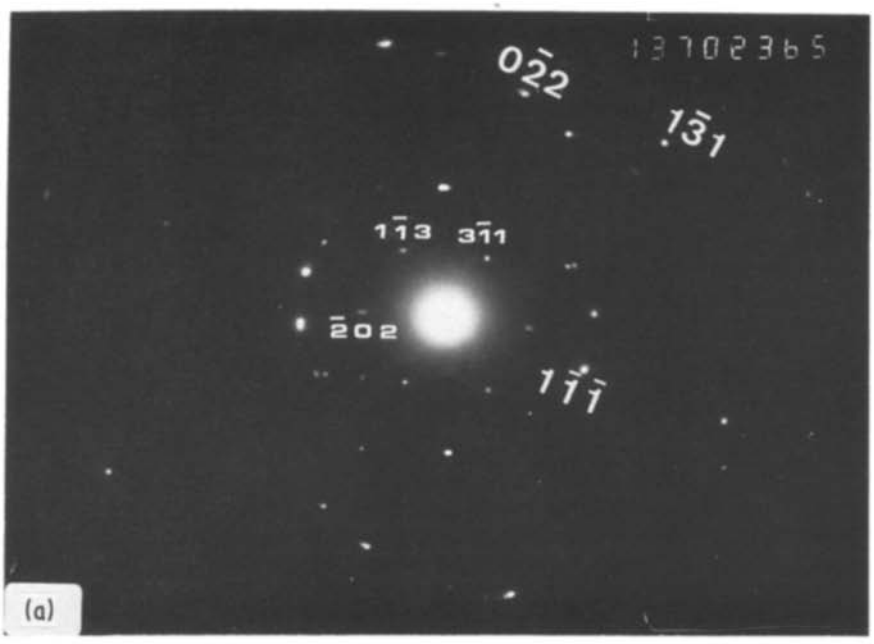

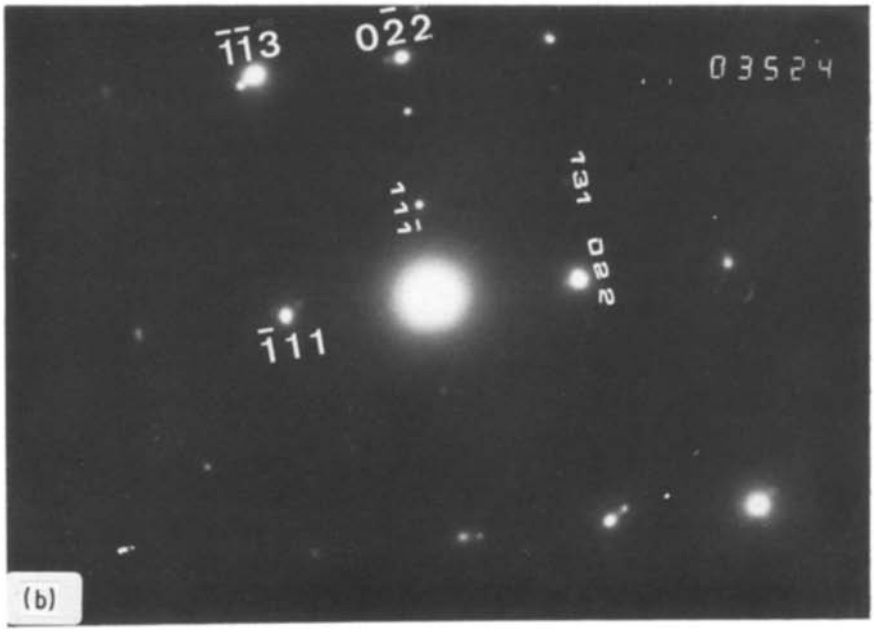

Figure 2 Electron diffraction patterns corresponding to: (a) Fig. 1d, (b) Fig. 1e.

3.1.2. δ'-phase formation

Homogeneous precipitation of $\delta'(Al_3Li)$ phase particles with diameters up to 4 nm was first observed immediately after melt quenching and refrigerating in liquid nitrogen, Fig. 3a. The presence of these particles was not affected by the grain boundary. Ageing at 200° C was characterized by rapid coarsening of δ' with a corresponding widening of the PFZs. In the vicinity of the PFZs, the number of precipitates per unit volume increased to a maximum after 16 h ageing as is evident from Fig. 3b. The wide variation in the δ'-particle size indicates that δ' nucleation is occurring during ageing as well as during the breakdown of the solid solution. At ageing temperatures below 200° C, the δ' was resolvable in the electron microscope. Above 200° C, the δ' coarsened more quickly. The coarsening behaviour of δ' is documented in Table I and the results are also represented graphically in Fig. 4. The coarsening rates deduced from this figure are listed in Table II. It is seen from this table that the coarsening rate of δ' precipitates in the present work at 200° C is above seven times that in ingot metallurgy Al–3% Li alloy while it is twice that in Al–4% Li. On the other hand, the achievable coarsening rate of δ' at 240° C seems to be nine times that reported by Baumann and Williams [10] and six times that obtained by Noble and Thompson [4] for Al–4% Li alloy.

The growth rate of the mean precipitate radius, r, is related to ageing time by the relation,

$$r^3 - r_0^3 = \alpha t$$

where r_0 is the initial particle radius ~ 3 nm. Plotting the natural logarithm of the slope of the curves in Fig. 4 against $1/T$ gives an activation energy of about 145 kJ mol^{-1}. This value is somewhat higher than that reported by Jensrud and Ryum [6] for the coarsening of δ' in Al–3 wt % Li alloy made by classical casting (130 kJ mol^{-1}). This difference arises from the fact that the volume fraction of the PFZ is much higher in the present case than in theirs, which causes a packing

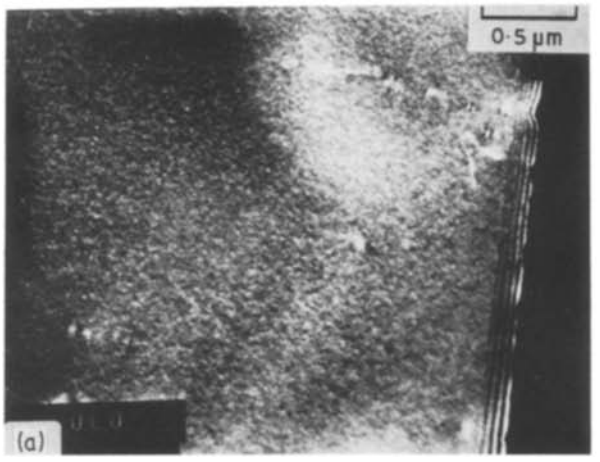

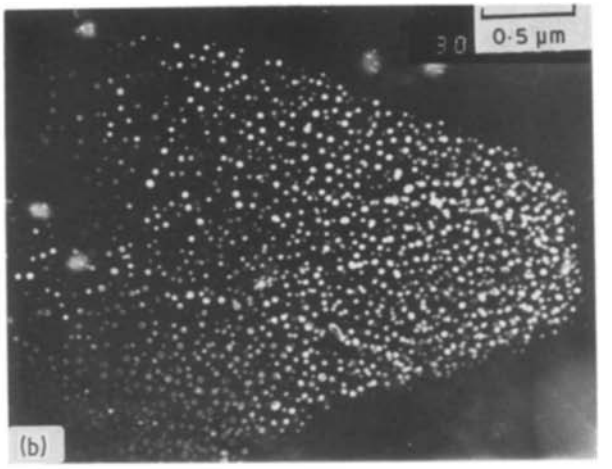

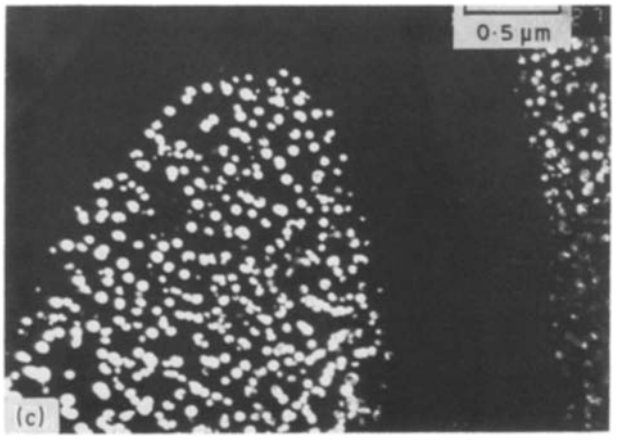

Figure 3 Dark-field micrograph imaged on a δ'-reflection: (a) as-melt-spun; (b) 200° C, 16 h; (c) 200° C, 100 h.

of δ' particles with the grains and affects their coarsening behaviour. This point will be discussed in more detail later.

Baumann and Williams [10] have analysed the growth of spherical particles of δ' on the basis of bulk diffusion using the formula proposed by Aaron *et al.* [11] that

$$r = \lambda(Dt)^{1/2}$$

where λ is a constant for a given solution-treatment condition and alloy composition and is a function of the supersaturation of the matrix in lithium, and D is the coefficient of diffusion of the solute atoms of lithium in the matrix. Fig. 5a reveals that coarsening of δ' takes place by selective growth of the larger precipitates (indicated by arrows) which is controlled by the diffusion of lithium to the δ'. With more prolonged ageing at 200° C and because of a very high volume fraction of δ' particles (apparently 47%), coalescence of δ' particles occurs, as shown in Fig. 5b.

On a quantitative metallographic basis, Baumann and Williams [12] have described the distribution of δ' particles. The volume fraction (V_v) of δ' is given by

$$V_v = -\ln(1 - A)\frac{4r}{3r + 3t}$$

where A is the area fraction of δ', r is the mean δ' particle radius, t is the foil thickness and V is the volume of the area under investigation. Also, the particle number density (N_v) can be expressed as follows:

$$N_v = \frac{N}{V}\left(\frac{t}{t + 2r}\right)$$

where N is the total number of particles imaged in a volume V. Applying this method in our work yielded higher values than those theoretically calculated (see Table III). The present results are also depicted graphically in Fig. 6, as a function of the cube root of time. From this figure, it appears that the volume fraction of δ' increases linearly after a period of ageing, 1 h. The difference between the expected and the calculated values of δ' volume fraction is due to the large PFZ volume fraction with respect to the grain size ($\sim 8\,\mu$m after ageing at 240° C for 120 h). This results in the packing of δ' particles with a consequent increase in N and hence their relative V_v, neglecting at the same time the discontinuity of δ' particles. A necessary correction should be introduced concerning both the real A and V with respect to grain surface and grain volume.

For ageing at temperatures close to the δ' solvus, precipitation took place entirely on dislocations, as

TABLE II Coarsening rates of δ' precipitates

Ageing temperature (° C)	Coarsening rate ($m^3 h^{-1}$)			
	Present work	Al–3% Li		Al–4% Li [2]
		[3]	[10]	
25	2.3×10^{-30}	–	–	–
160	5.3×10^{-25}	–	–	–
200	3.5×10^{-24}	3.9×10^{-25}	–	4.5×10^{-25}
240	10^{-23}	–	1.6×10^{-24}	6.2×10^{-24}
280	4×10^{-23}	–	–	–
300	2×10^{-23}	–	–	–

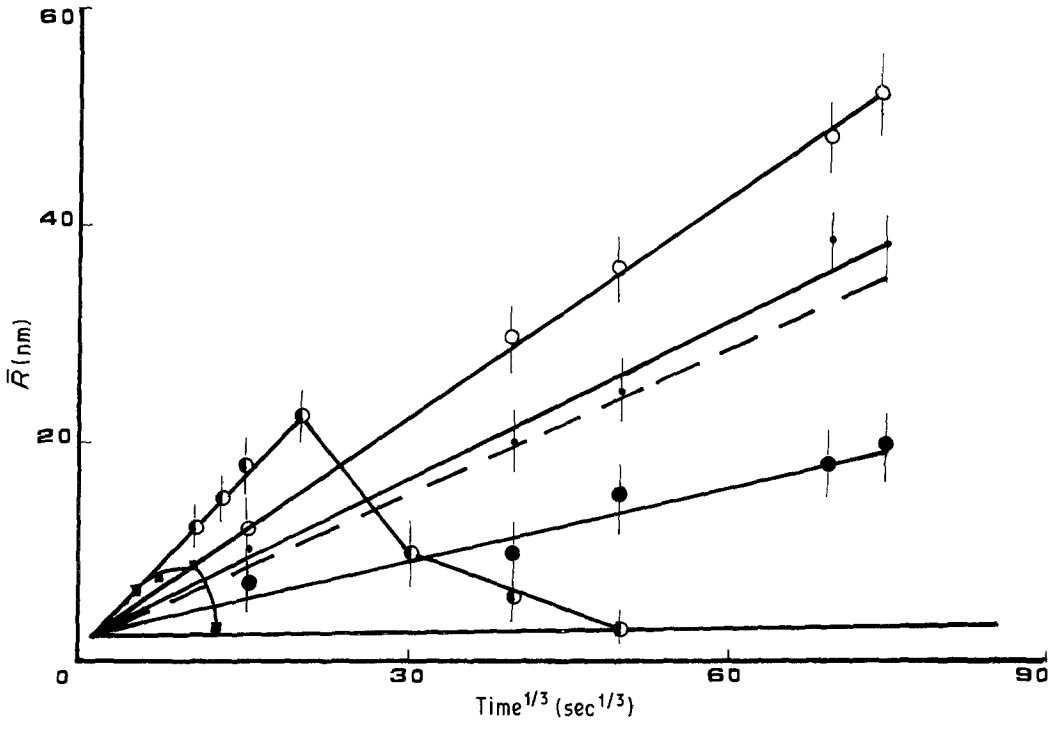

Figure 4 Coarsening of δ'-phase particles as a function of cube root of ageing time. (●) 160° C, (●) 200° C, (○) 240° C, (◐) 280° C, (■) 300° C. (– – –) 200° C [3], (——) 25° C.

shown in Fig. 7. As can be seen from this micrograph, there is a gradient of δ' particle sizes that develops during ageing. According to Baumann and Williams [12], the vacancy-depleted regions near dislocations should develop smaller particles than the highly vacancy supersaturated regions remote from dislocations. At high temperatures the diffusivity gradient will not disappear immediately and a particle size gradient will be maintained.

The PFZ growth rate is shown in Tables Ia to f and graphically in Fig. 8. The relationship between the PFZ half-width ($\omega/2$) and annealing time (t) is given by,

$$\omega/2 = k(t)^{1/3}$$

where k is the growth constant. The results of Sanders *et al.* [3] on Al–2.8% Li–0.3% Mn alloy with an initial grain size of the order of 100 μm subjected to ageing at 200° C are superimposed in Fig. 9 for comparison. As can be seen, the width of the PFZ has not been influenced by the grain refinement enhanced by rapid solidification. As a consequence, the volume fraction of PFZ should be considerably higher than

TABLE III Variation of δ' volume fraction with ageing temperature

Temperature (° C)	Maximum solubility of Li (wt %)	Available Li (wt %)	Maximum δ' (vol %)
25	1.2	1.36	30
160	1.55	1.06	25
200	1.61	0.95	24
240	1.8	0.76	21
280	2.0	0.56	18
300	2.09	0.47	
320	2.22	0.34	

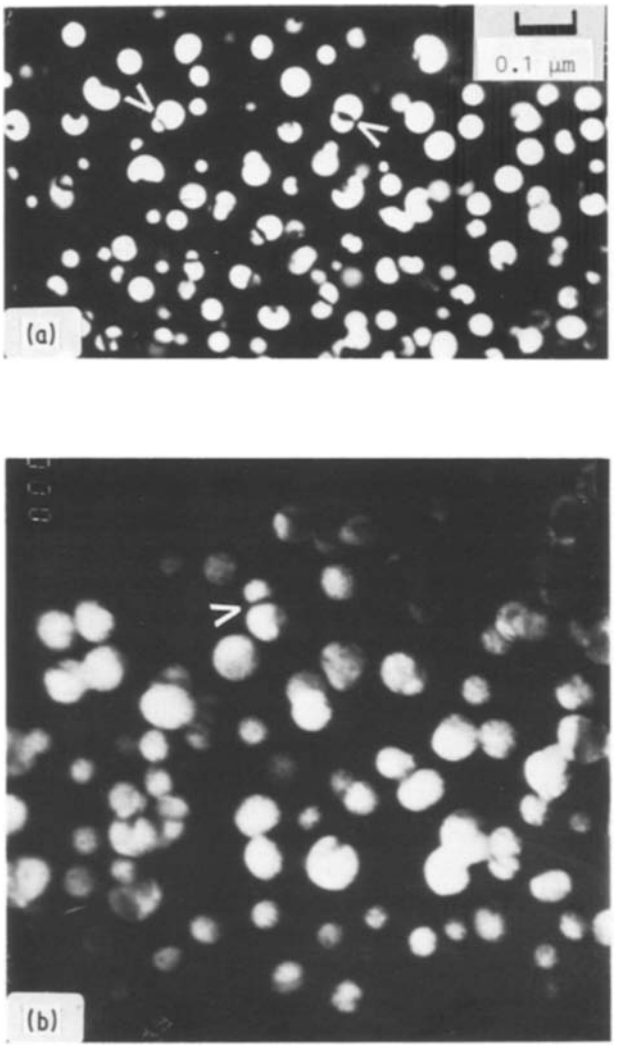

Figure 5 Dark-field micrographs showing coarsening and coalescence of δ' at 200° C after prolonged ageing: (a) 100 h, (b) 120 h.

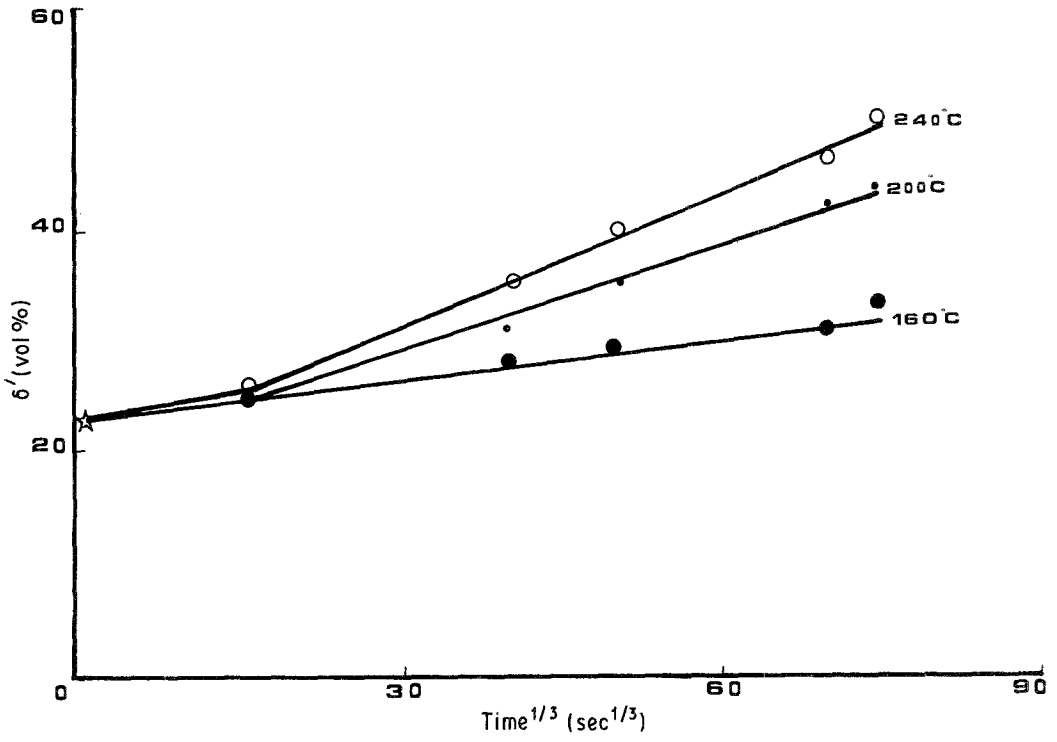

Figure 6 Variation in the δ'-volume fraction as a function of cube root of ageing time.

that expected in the case of classical casting as is demonstrated by Fig. 9, where the volume fraction of PFZ is found to be of the order of 60% following ageing at 240° C for 120 h. The continuity of the soft areas is considered to be a good factor in contributing to the alloy ductility as will be discussed in the next section.

3.1.3. $\delta' \rightarrow \delta$ transformation

Shchegoleva and Rybalko [13] have proposed that the transformation from fcc (δ') to bcc (δ) is of martensitic type. Failure to produce diffraction evidence for the formation of δ by this mechanism raises strong doubts about its possibility. Furthermore, such a transformation would imply that the size of the newly formed δ would be equal to that of the parent δ', which has not yet been reported. Venables *et al.* [14] have found that δ nucleates, rather, on high-energy sites such as grain boundaries at lower ageing temperatures and in the matrix on dislocations and on the more highly strained δ'/matrix interface at higher temperatures.

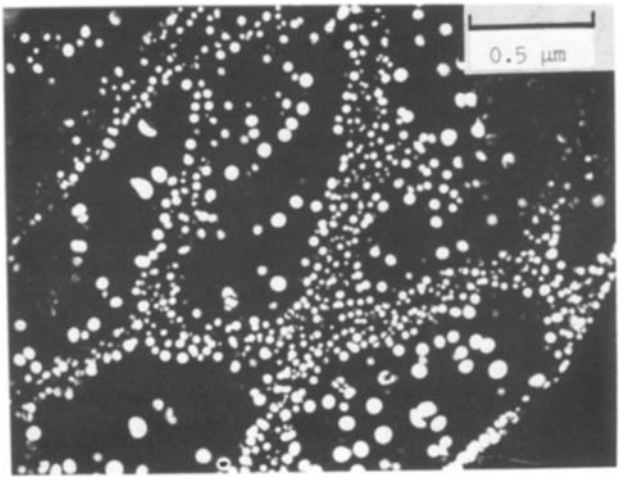

Figure 7 Heterogeneous growth of δ' particles (280° C, 5 min).

Fig. 10a, which is a dark-field micrograph imaged on a δ/δ' superimposed reflection, shows the microstructure following ageing at 280° C for 15 min. In this micrograph, a fairly coarse particle of δ-phase is seen surrounded by relatively fine particles of δ'-phase. Some of the δ' particles are seen on the top surface of the δ particle. Increasing the ageing time up to 30 min resulted in the formation of a δ' precipitate-free-zone around the δ particle, leading to the conclusion that the δ-phase grows by dissolution of nearby δ'. This point is best seen in Fig. 10c, corresponding to an intermediate ageing time between Figs 10a and b. Around each particle of δ is a region of very fine δ' particles. This observation is explicable in terms of the dissolution of δ' particles in the matrix which increases the concentration of lithium in this area above the maximum solubility (see Table III). As a result, a breakdown of the matrix takes place giving rise to the formation of such precipitates in a manner similar to that shown in Fig. 3a. We believe that δ particles nucleate in the strain field around the δ' particle on ageing at temperatures as high as 280° C.

Based on the data listed in Tables Ie and f, it would seem that at 280° C the size of δ increases up to 2 h and then remains reasonably constant up to 36 h, whilst the number of δ precipitates goes on increasing as revealed from Figs 11a and b. At 300° C the size increases with time (up to 1 h) whilst the number remains constant. The δ-phase particles have a regular shape which is almost spherical. A higher ageing time at this temperature or increasing the ageing temperature to 300° C changes the form to rod/plate-shaped. Figs 12a and b, (310° C, 1 h), indicate that coarsening takes place by the joining of more than one particle

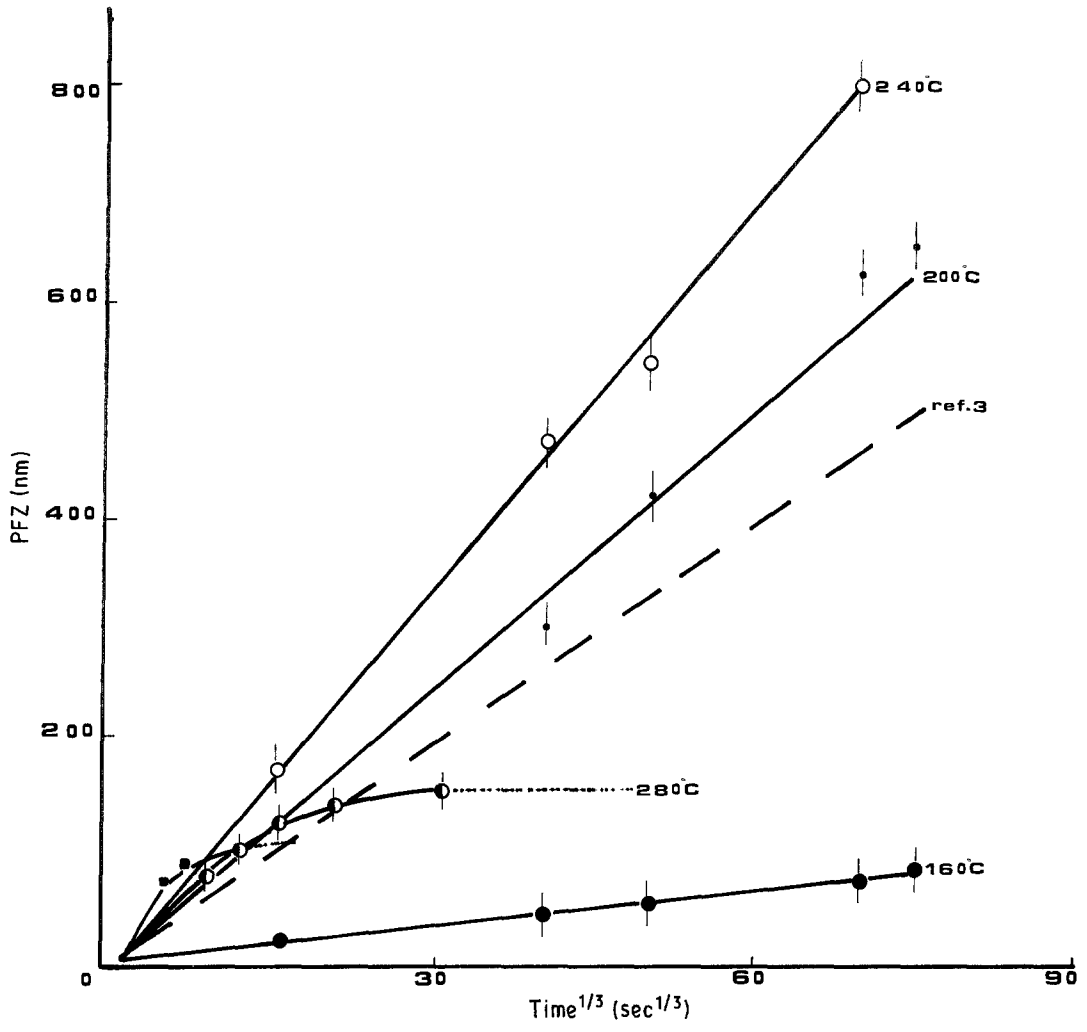

Figure 8 Widening of PFZ half width as a function of cube root of ageing time. (···) $\alpha + \delta' \rightarrow \alpha + \delta$.

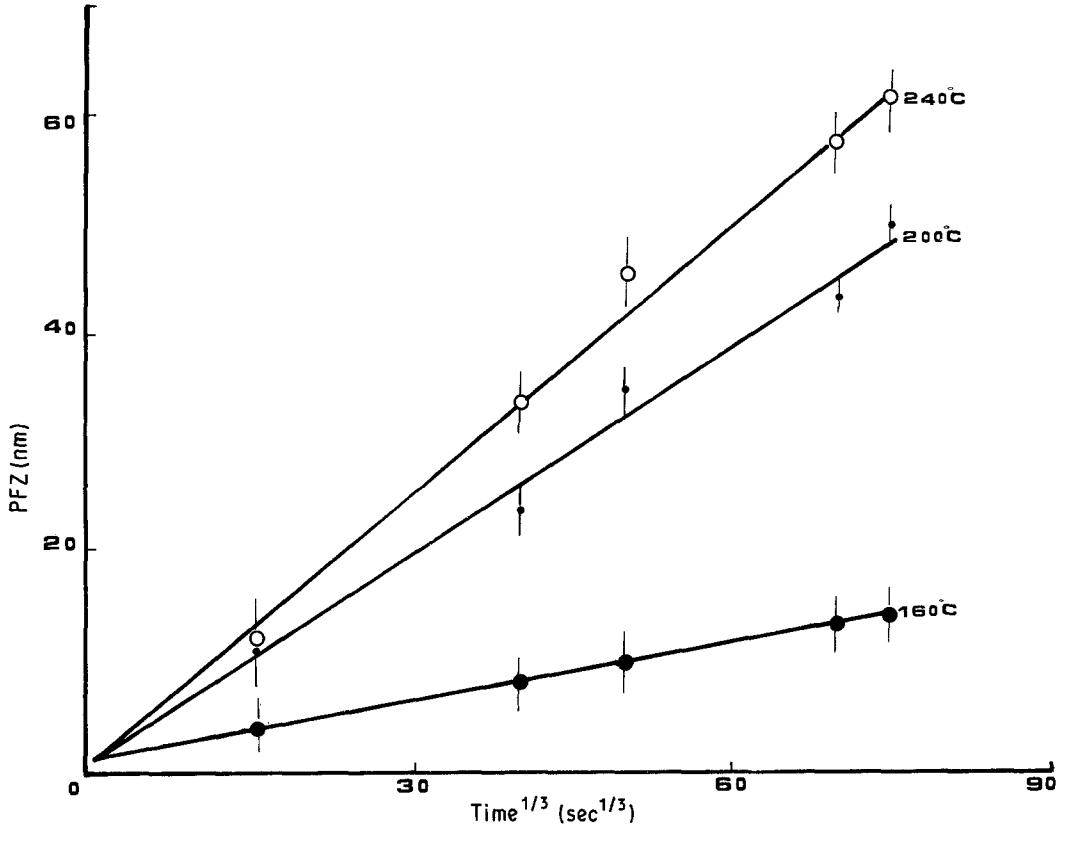

Figure 9 Variation in the PFZ volume fraction as a function of cube root of ageing time.

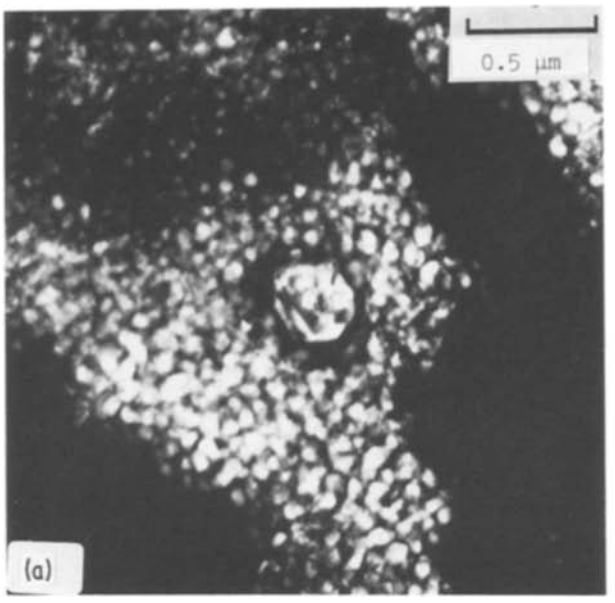

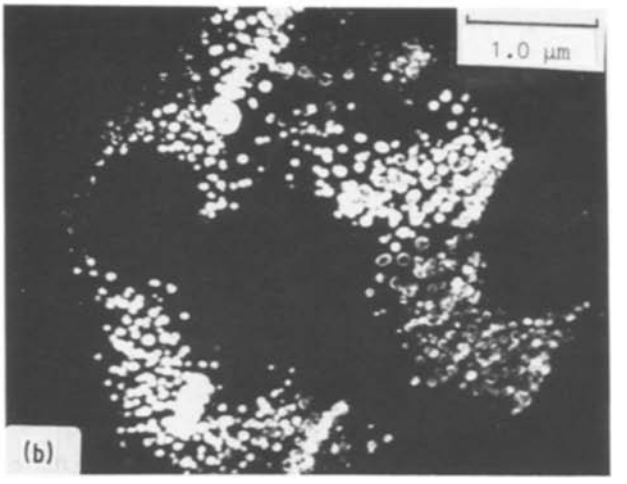

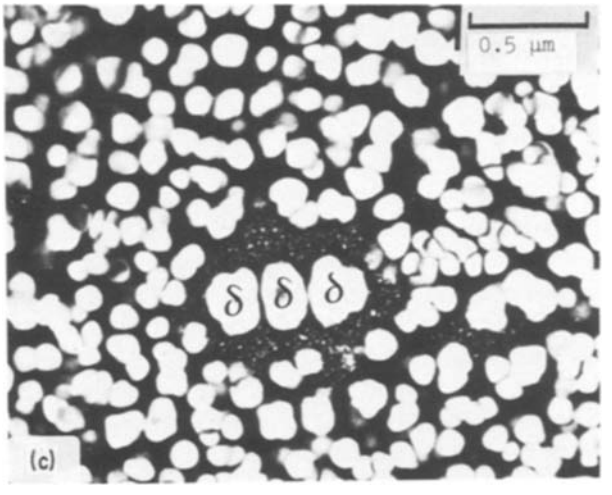

Figure 10 Dark-field micrographs imaged on a δ' or δ'/δ superimposed reflection showing the formation of δ particles in a matrix of δ' particles: (a) 280° C, 15 min; (b) 280° C, 1 h; (c) 280° C, 30 min (δ particles are marked).

with a clean interface boundary as indicated by the presence of dislocation arrays (arrowed). The existence of dislocations around each particle of δ-phase in Fig. 12a suggests that in this condition, the δ particles are coherent or at least semi-coherent. Table If and Fig. 4, also draw attention to the fact that the δ' particle size reaches its maximum on ageing at 280° C after 2 h, beyond which it falls rapidly because of the increase in the number of δ particles at the expense of the dissolution of δ' particles. On the other hand, coarsening of δ' at 300° C reaches a maximum after 15 min with a particle diameter close to that obtained at 240° C after the same ageing time.

3.2. Mechanical properties

The changes in the hardness of as-melt-spun ribbons on ageing at 160, 200 and 280° C are reported in Table II. The peak hardness is obtained by ageing at 200° C with an ageing time ~ 16 h. Ageing at higher temperatures, i.e. 280° C, exhibits a significant hardening response for short ageing times (~ 1 h) whereas ageing for longer times is accompanied by drastic softening. On the other hand, ageing at lower temperatures i.e. 160° C, exhibits a smooth increase in the hardness. These results are in good agreement with our

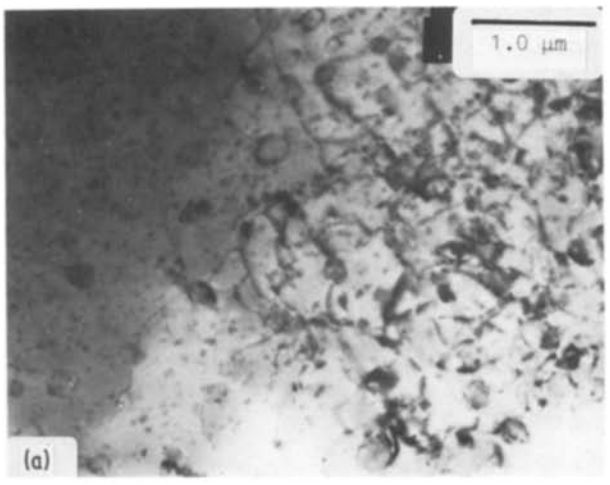

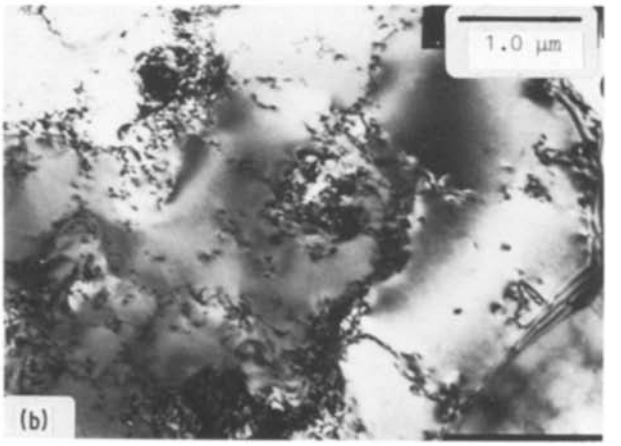

Figure 11 Transmission electron micrographs showing the growth of δ particles as well as the increase in their number as a function of ageing time at 280° C: (a) 36 h, (b) 100 h. Note the formation of dislocations around the δ particles and the disappearance of δ' particles.

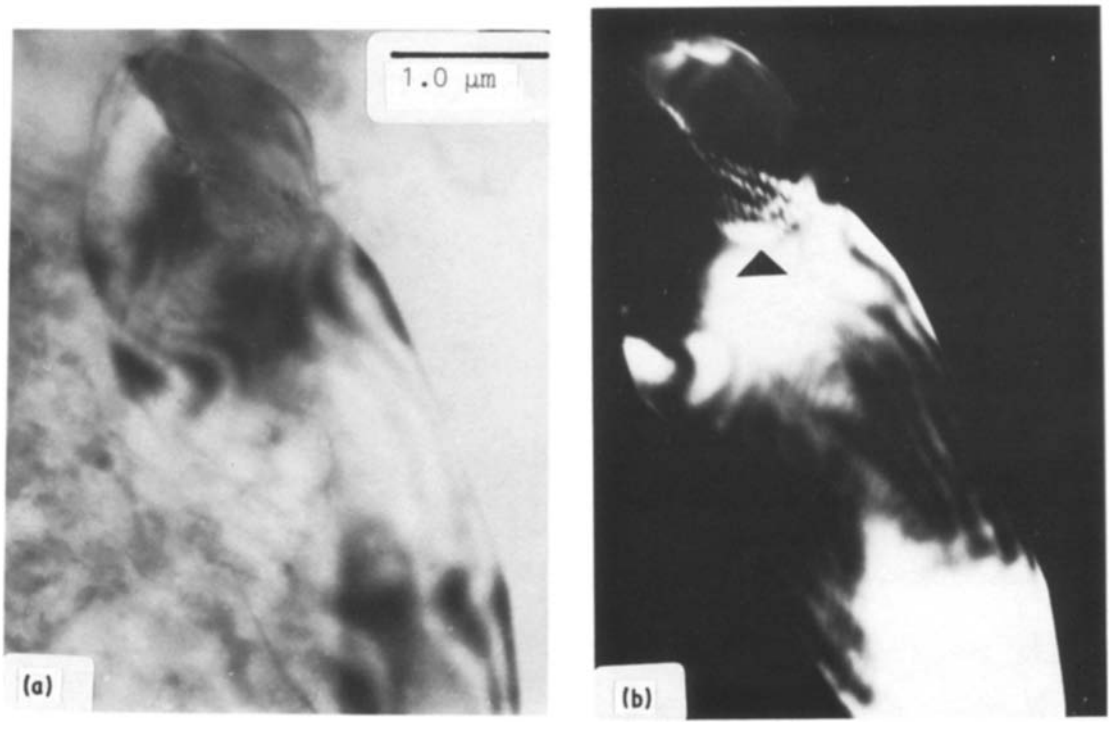

Figure 12 Transmission electron micrographs showing the agglomeration of δ particles on ageing in the (α + δ) region: (a) bright field, (b) dark field.

microstructural observations on the precipitation and coarsening behaviour of δ' explained in Table I. Comparing our results with the work of Webster *et al.* [15] made on Al–2.7% Li compacted powders, shows that peak hardness in their work was obtained at 450 K (177° C) for an ageing time of 30 h. Noble and Thompson [2] have found that maximum strengthening in Al–3 wt % Li solid state alloy is produced by the δ' when its diameter is $\sim$ 30 nm. Ageing at temperatures above 200° C leads to the rapid coarsening of the precipitate to a size $\sim$ 30 nm, causing a decrease in hardness. In view of the above data, it may be said that the major part of hardening is due to the particle size and volume fraction of δ', while the effect of grain-size refinement appears in accelerating the ageing time at which peak hardening takes place. This may be due to the formation of noticeable PFZ areas which contribute to alloy softening.

Table IV summarizes the mechanical properties of the present consolidated powder materials, following different heat treatments. It is found that solution heat treatment for 0.5 h at 540° C is sufficient to dissolve all the coarse δ and δ' particles to enrich the matrix with solute atoms of lithium. This results in a visible improvement in both the strength and ductility of the alloy. Typical stress–strain curves obtained from aged specimens are demonstrated in Figs 13a and b. Deformation beyond the yield limit at both ageing temperatures leads to a substantial increase in the work-hardening rate due to creation of a considerable amount of dislocations. However, the presence of δ' particles tends to retard the motion of dislocations and hence reduce their velocity. This effect depends on the type of δ', i.e. whether they are shearable or non-shearable, which, in turn, depends on their radius and interparticle distance. From the slope of the straight portion of these curves, the values of the Young's modulus, E, were calculated and are listed in Table IV. It is found that the contribution of lithium in solid solution represents 80% of the total increase in E as compared to pure aluminium whereas the effect of the precipitation of δ' represents only 20% [16]. The strength–ductility relationships for the powder metallurgy alloy evaluated on the present program are

TABLE IV Mechanical properties of powder metallurgy alloy

Solution treatment	Ageing treatment	$\sigma_{0.2}$ (MPa)	σ_m (MPa)	Elongation (%)	E (GPa)	$\Delta E/E^*_{Al}$
As-extruded	–	72	196	17	78.5	19
540° C/0.5 h	–	105	234	19	79.8	21
	200° C/14 h	390 (256)	419 (385)	5 (8)		
	200° C/16 h	372	440	5	81.9	24
	200° C/20 h	366	432	6		
	200° C/24 h	367 (264)	430 (376)	4.5 (5)		
	220° C/14 h	314	384	7		
	220° C/16 h	310	387	7.5	82.5	25
	220° C/20 h	311	386	6.5		
	220° C/24 h	266	356	10.5		

* E_{Al} = 66 GPa.
Figures quoted in brackets are taken from [3].

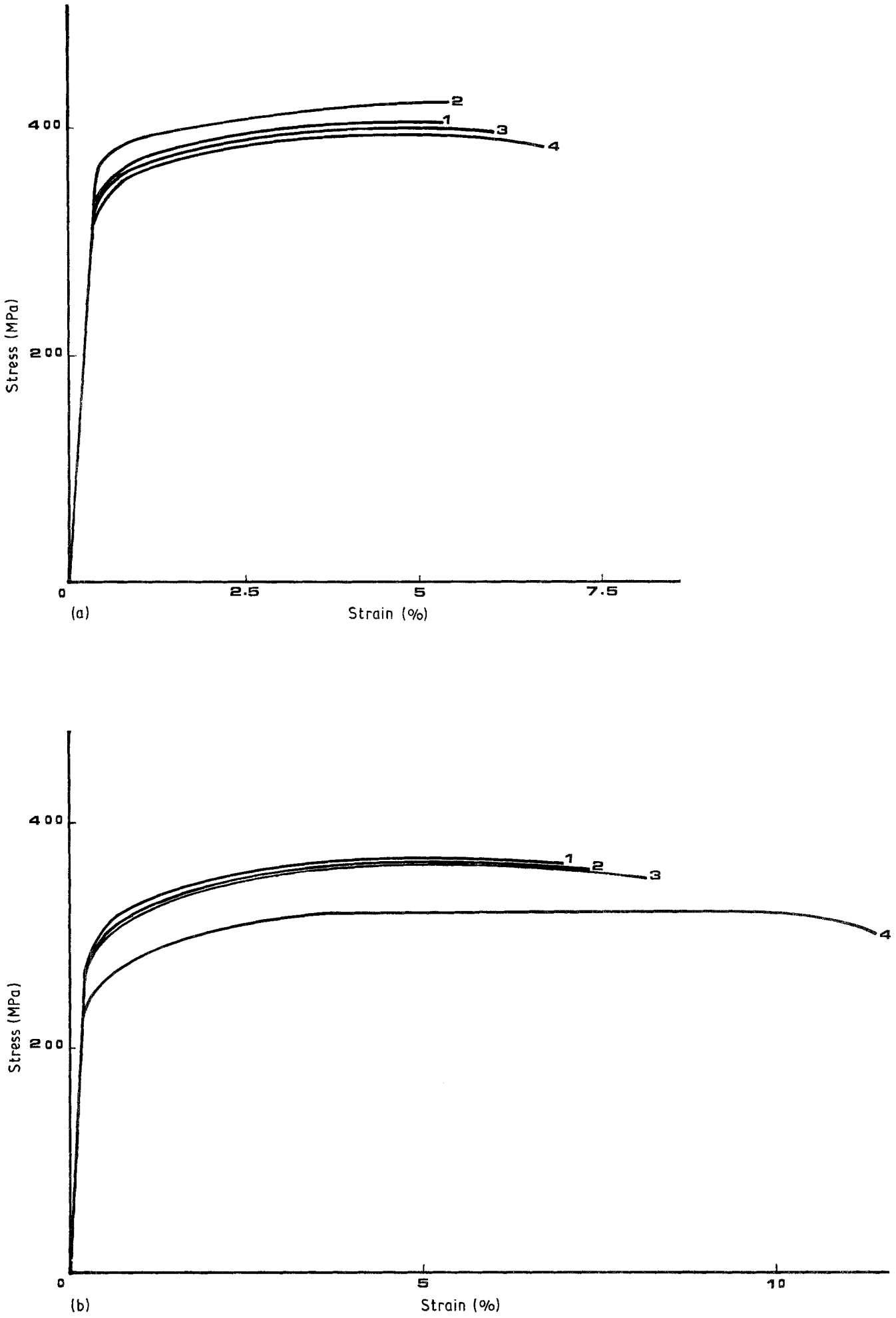

Figure 13 Stress–strain curves following ageing at (a) 200° C, (b) 220° C. (a) 1, 12 h; 2, 16 h; 3, 20 h; 4, 24 h. (b) 1, 14 h; 2, 16 h; 3, 20 h; 4, 24 h.

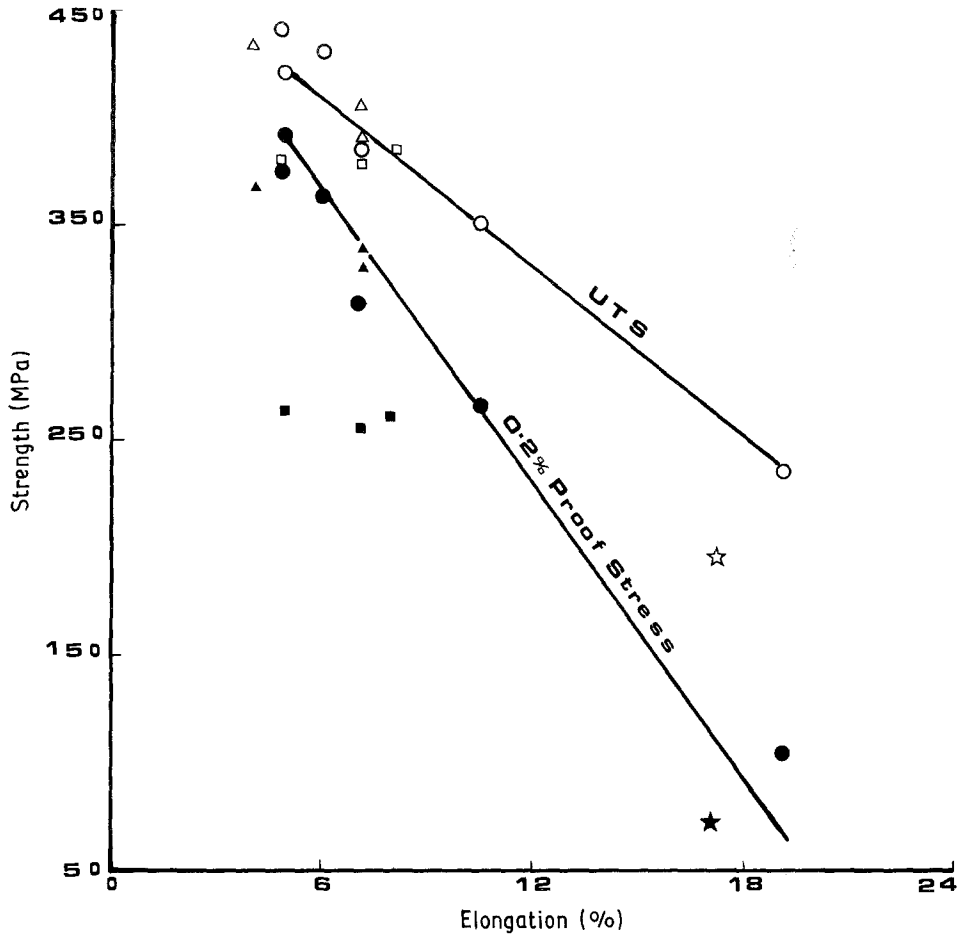

Figure 14 Strength–ductility relationship for solution heat-treated powders following ageing at 200 and 220° C. Points marked by stars represent the as-extruded powders. (△, ▲) [15], (□, ■) [3].

compared in Fig. 14. All the spots virtually fall on two straight lines, one for σ_m and the other for $\sigma_{0.2}$. The results produced by Webster *et al.* [15] on Al–3% Li powder metallurgy alloy with a grain size of about 5 μm which is almost the same as in our case, are superimposed for comparison. The use of rapidly cooled powder for producing Al–Li alloys appears in the reasonable improvement in yield strength ($\sim$ 100 to 130 MPa) above that obtained from ingot metallurgy alloy [3] with an initial grain size of about 100 to 150 μm. Because of the large volume fraction of precipitate free zone, approximately 32% for an ageing treatment at 220° C for 24 h as estimated from Fig. 9, a good ductility, $\sim$ 11%, is achieved, which is reasonably higher than that expected from ingot metallurgy alloys [5].

4. Conclusions

Rapid solidification of Al–2.5% Li results in a drastic refinement of the grains ($\sim$ 2 μm against 150 μm for ingot metallurgy alloy). Ageing this alloy at temperatures below the $\delta'(Al_3Li)$ solidus line results in the formation of PFZs with the same widths as the counterpart ingot metallurgy alloy. Thus, the PFZ volume fraction is about 60% in MS alloys as compared to 4% for IM alloy. Also, because of packing of δ' particles within the grains, the calculated volume fraction is much higher than that expected from the Baumann and Williams model. The equilibrium phase δ(AlLi) seems to occur at the grain boundaries at lower ageing temperatures and in the matrix on dislocations and on the δ'/matrix interface at higher temperatures. The growth of particles is attributed to the dissolution of nearby δ' particles. The use of rapid solidification appears in the reasonable improvement in yield strength ($\sim$ 130 MPa) above that obtained for ingot metallurgy alloy. Because of the large volume fraction of PFZ, a good ductility $\sim$ 11% can be achieved with a UTS of the order of 356 MPa.

References

1. K. K. SANKARAN and N. J. GRANT, *Mater. Sci. Engng* **44** (1980) 213.
2. B. NOBLE and G. E. THOMPSON, *Met. Sci. J.* **5** (1971) 114.
3. T. H. SANDERS, Jr., E. A. LUDWIEZAK and R. R. SAWTELL, *Mater. Sci. Engng* **43** (1980) 247.
4. D. B. WILLIAMS, Proceedings 1st International Aluminium–Lithium Conference, Stone Mountain, Georgia, May 1980 (The Metallurgical Society of AIME, Warrendale, Pennsylvania, 1981) p. 89.
5. T. H. SANDERS Jr and E. A. STARKE Jr, *Acta Metall.* **30** (1982) 927.
6. O. JENSRUD and N. RYUM, *Mater. Sci. Engng* **64** (1984) 229.
7. G. W. LORIMER and R. B. NICHOLSON, *Acta Metall.* **14** (1966) 1009.
8. J. M. SILCOCK, *J. Inst. Metals* **88** (1959/60) 357.
9. C. L. ANGERMANN, *J. Nucl. Mater.* **11** (1964) 41.
10. S. F. BAUMANN and D. B. WILLIAMS, *Met. Trans. A* **16A** (1985) 1203.
11. H. B. AARON, D. FAINSTEIN and G. R. KOTLER, *J. Appl. Phys.* **41** (1970) 4404.

12. S. F. BAUMANN and D. B. WILLIAMS, *Acta Metall.* **33** (1985) 1069.
13. T. V. SHCHEGOLEVA and O. F. RYBALKO, *Phys. Met. Metallogr.* **42** (1976) 83.
14. D. VENABLES, L. CHRISTODAULOU and J. R. PICKENS, *Scripta Metall.* **17** (1983) 1263.
15. D. WEBSTER, G. WALD and W. S. CREMENS, *Met. Trans. A* **12A** (1981) 1495.
16. B. NOBLE, S. J. HARRIS and K. DINSDALE, *J. Mater. Sci.* **17** (1982) 461.

Received 27 August 1986
and accepted 4 March 1987